UCRL-JC-130448
PREPRINT

On Electromagnetic Acceleration of Material from a Plate Hit by a Pulsed Electron Beam

Manuel Garcia

**This paper was prepared for submittal to the
Intense Ion & Electron Beam Session
Institute for Electrical and Electronics Engineers
International Conference on Plasma Science
Raleigh, NC
June 1-4, 1998**

April 16, 1998

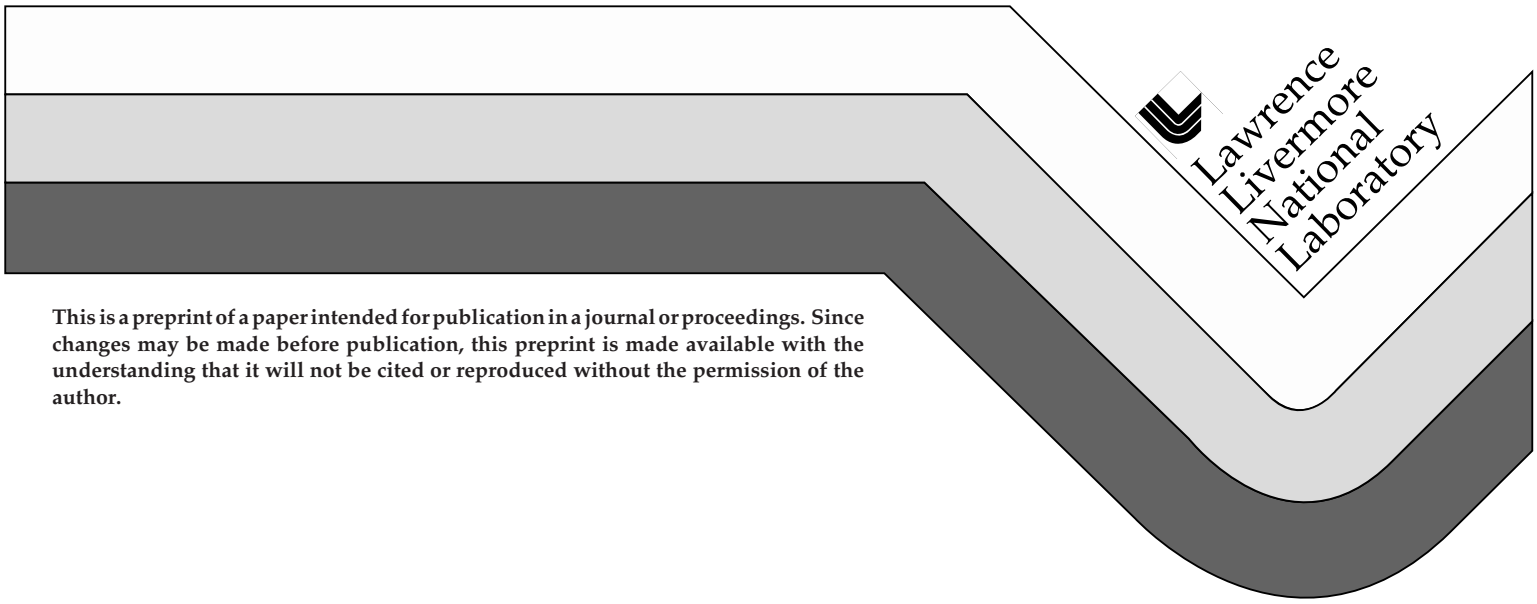

On electromagnetic acceleration of material from a plate hit by a pulsed electron beam

Manuel Garcia

16 April 1998

Lawrence Livermore National Laboratory, L-153, P.O. Box 808, Livermore CA 94550
garcia22@llnl.gov, (925) 422-6017, FAX: (925) 423-5080

An intense pulsed electron beam traversing a thin metal plate creates a volume of dense plasma. Current flows in this plasma as a result of the charge and magnetic field introduced by the relativistic electrons. A magnetic field may linger after the electron beam pulse because of the conductivity of the material. This field decays by both diffusing out of the conducting matter and causing it to expand. If the magnetized matter is of low density and high conductivity it may expand quickly. Scaling laws for this acceleration are sought by analyzing the idealization of a steady axisymmetric flow. This case simplifies a general formulation based on both Euler's and Maxwell's equations. As an example, fluid with conductivity $\sigma = 8 \times 10^4$ Siemens/m, density $\rho = 8 \times 10^{-3}$ kg/m^3, and initially magnetized to $B = 1$ Tesla can accelerate to $v = 10^4$ m/s within a distance comparable to $L = 1$ mm and a time comparable to $\sigma\mu L^2 = 100$ ns, which is the magnetic diffusion time. If instead, $\sigma = 8 \times 10^3$ Siemens/m and $\rho = 8 \times 10^{-5}$ kg/m^3 then $v = 10^5$ m/s with a magnetic diffusion time $\sigma\mu L^2 = 10$ ns. These idealized flows have $R_M = \sigma\mu vL = 1$, where R_M is the magnetic Reynolds number. The target magnetizes by a thermal electric effect.

---

1) Motivation for this study

An electron beam accelerator is being designed for the purpose of generating an x-ray pulse train of great intensity from a metal target. This work involves a number of DOE laboratories. Of concern is how the outflow of material from this target may degrade the radiation pulse train by interfering with the trajectories of the accelerated electrons. Three types of outflow are possible: 1) prompt

ejection of positive ions during the course of any pulse, see References 1—3, 2) electromagnetic acceleration of target material, and 3) thermal acceleration of target material, see References 4—8.

The most significant effect to the target is the removal of material by thermal acceleration — this leaves a hole in the plate. The volume of material heated by the electron beam exhausts into a vacuum and reaches a maximum velocity of twice the initial speed of sound, typically near 10 mm/μs (10 km/s). The suddenness of the expansion can lead to a departure from thermal equilibrium between the neutral and ionized portions of the flow. Of the three outflow mechanisms noted in the previous paragraph, this effect is the one most clearly observed and calculated, see References 4—8.

Experiments are being conducted at the Integrated Test Stand (ITS) accelerator at the Los Alamos National Laboratory, and the Experimental Test Accelerator II (ETA-II) at the Lawrence Livermore National Laboratory to establish beyond doubt the presence of "positive ion backstreaming" during the course of a single electron beam pulse. These are challenging experiments. A physical consequence of ion backstreaming is that the electron beam approaching the target plate will experience a reduction of its space charge, and pinch as a result of its own $\mathbf{j} \times \mathbf{B}$ force. The pinched beam reaches a minimum diameter and then expands before striking the target. The expectation is that the spot size at the target will grow during the course of the pulse, and the intensity of the resulting x-ray emission will diminish. Experiments are aimed at measuring these changes in spot size and intensity. Ion backstreaming is expected to be the earliest and fastest material ejection, with a velocity as high as 10 m/μs (10^4 km/s). See References 1—3. It appears that a superthermal outflow of plasma may have been observed by a microwave interferometer measuring electron density upstream of the target, this work is to be presented later this year, see Reference 9.

This report describes the possibility of electromagnetic acceleration of neutral conducting material from the target. Can plasma leave the target at speeds expected for ion backstreaming? If so then the electron beam might not pinch as anticipated. My first attempt to quantify this effect was far too speculative (noted as Reference 10), but it lead to the work to be presented here, in which every effort has been made to be methodical and rigorous.

The plan of this report is as follows. General equations for the motion of an inviscid conducting fluid with embedded sources of current and charge — the electron beam — are formed by combining Maxwell's equations and the Euler equation with a Lorentz force. This occupies sections 2—6 of this report. A flow that can be described easily is presented in section 7, it involves the steady motion of an incompressible, conducting fluid with an initial magnetic field and no source terms. This flow is an idealization where conducting fluid retains a magnetization after the passage of an electron beam pulse. In section 8, the velocity and magnetic field are solved as functions of distance from the plate for the specific case of axisymmetric flow with azimuthal magnetic field. Two numerical examples of this case are shown in section 9. Section 10 is a discussion of the effects of conductivity, density, and initial magnetization upon the ultimate fluid speed. Section 11 describes how the target initially magnetizes. Section 12 states conclusions. The Appendix describes charged flow.

2) Governing equations

Consider an electron beam as a source of pulsed charge density $\rho_0(\mathbf{r}, t)$ and current density $\mathbf{j}_0(\mathbf{r}, t)$ within a conducting fluid. Maxwell's equations follow,

$$\text{div } \mathbf{D} = \rho_0(\mathbf{r}, t), \tag{1}$$

$$\text{curl } \mathbf{E} = -\frac{\partial \mathbf{B}}{\partial t}, \tag{2}$$

$$\text{div } \mathbf{B} = 0, \tag{3}$$

$$\text{curl } \mathbf{H} = \mathbf{j}_T + \frac{\partial \mathbf{D}}{\partial t}. \tag{4}$$

The constitutive relations are:

$$\mathbf{D} = \varepsilon \mathbf{E}, \tag{5}$$

$$\mathbf{B} = \mu \mathbf{H}, \tag{6}$$

where $\varepsilon = 8.854 \times 10^{-12}$ farad/m, and $\mu = 4\pi \times 10^{-7}$ henry/m, the permeability of non-magnetic material.

The total current density $\mathbf{j}_T(\mathbf{r}, t)$ is the sum of the electron beam current density and current flow in the conducting fluid,

$$\mathbf{j}_T = \mathbf{j}_0 + \mathbf{j} = \text{curl}\,\frac{\mathbf{B}_0}{\mu} + \sigma(\mathbf{E} + \mathbf{v} \times \mathbf{B}). \tag{7}$$

The electron beam current density within the fluid is equivalent to the curl of a source magnetic induction $\mathbf{B}_0(\mathbf{r}, t)$. Current flow in the fluid is assumed to follow an Ohm's law with a single velocity parameter. The implicit assumption here is that any difference in the drift velocities of electrons and positive ions, which is required to produce current, is small in comparison to their motion with the material. This is true if the physical scale of the system is large, or if the electron density is large, see Reference 11 for a discussion of this point.

If ρ is the mass density, the hydrodynamic equation of continuity is

$$\frac{\partial \rho}{\partial t} + \text{div}(\rho \mathbf{v}) = 0. \tag{8}$$

The momentum equation is

$$\rho\left(\frac{\partial \mathbf{v}}{\partial t} + \mathbf{v} \cdot \nabla \mathbf{v}\right) = -\nabla p + \mathbf{j} \times \mathbf{B}. \tag{9}$$

The conducting fluid moves in response to a pressure gradient, a result of heating by the electron beam, and its own Lorentz force. This is an ideal fluid, viscosity and thermal conductivity are absent.

3) Current density

By combining equations (4) and (7), the current density in the fluid is seen to be

$$\mathbf{j} = \text{curl}\left(\frac{\mathbf{B} - \mathbf{B}_0}{\mu}\right) - \frac{\partial \mathbf{D}}{\partial t}, \tag{10}$$

and by taking the divergence of (10) with an eye to equation (1),

$$\frac{\partial \rho_0}{\partial t} + \text{div}(\mathbf{j}) = 0. \tag{11}$$

If the temporal variations of ρ_0 and $\mathbf{D}$ occur at a rate much lower than the plasma frequency of the material σ/ε they can be neglected, as neither relativistic mass flow nor electromagnetic waves are being considered. The current density $\mathbf{j} = \sigma(\mathbf{E} + \mathbf{v} \times \mathbf{B})$ arises to reduce the difference in the magnetic field $\mathbf{H} - \mathbf{H}_0 = (\mathbf{B} - \mathbf{B}_0)/\mu$ within the conducting fluid.

4) Scalar and vector potentials

By expanding equation (11) with the definition of $\mathbf{j}$, and assuming "slow" time variation as described in section 3, the following is determined,

$$\text{div}(\mathbf{v} \times \mathbf{B}) = \frac{-\rho_0}{\varepsilon}. \tag{12}$$

By expanding equation (2) with $\mathbf{E} = \mathbf{j}/\sigma - \mathbf{v} \times \mathbf{B}$, and using equation (10) for $\mathbf{j}$, the following is determined,

$$\text{curl}(\mathbf{v} \times \mathbf{B}) = \frac{\partial \mathbf{B}}{\partial t} - \frac{\nabla^2(\mathbf{B} - \mathbf{B}_0)}{\sigma\mu}. \tag{13}$$

The vector relation $\text{curl}[\text{curl}(\mathbf{A})] = \text{grad}[\text{div}(\mathbf{A})] - \nabla^2(\mathbf{A})$ was used to find equation (13). The cross product $\mathbf{v} \times \mathbf{B}$ can be defined in terms of a scalar potential ϕ and vector potential Ψ as follows,

$$\mathbf{v} \times \mathbf{B} = \nabla\phi + \nabla \times \Psi. \tag{14}$$

The divergence of (14) shows that

$$\nabla^2\phi = \mathrm{div}(\mathbf{v} \times \mathbf{B}), \tag{15}$$

and the curl of (14) shows that

$$-\nabla^2\Psi = \mathrm{curl}(\mathbf{v} \times \mathbf{B}), \tag{16}$$

where Ψ is assumed to have zero divergence. By comparing (12) with (15), and (13) with (16) it is seen that the scalar potential is a consequence of the charge density, while the vector potential arises from the diffusion of **B** through the conducting fluid. Notice that the diffusion of **B** is a process paced by the conductivity.

5) Uniform conductivity flow

A uniform conductivity, which could vary in time, has been assumed in the previous sections. The equations describing the flow of such a fluid, with parameters **v**, **B**, ρ, and p are (8), (12), (13), the momentum equation

$$\rho\left(\frac{\partial \mathbf{v}}{\partial t} + \mathbf{v}\cdot\nabla\mathbf{v}\right) = -\nabla p + \mathrm{curl}\left(\frac{\mathbf{B} - \mathbf{B}_0}{\mu}\right) \times \mathbf{B}, \tag{17}$$

and an equation of state $p(\rho)$.

6) Non-uniform conductivity flow

If the conductivity can vary spatially, then equation (12) is replaced by

$$\mathrm{div}(\mathbf{v} \times \mathbf{B}) = \frac{-\rho_0}{\varepsilon} - \frac{\mathrm{curl}(\mathbf{B} - \mathbf{B}_0)}{\sigma\mu} \cdot \frac{\nabla\sigma}{\sigma}, \tag{18}$$

and equation (13) is replaced by

$$\mathrm{curl}(\mathbf{v} \times \mathbf{B}) = \frac{\partial \mathbf{B}}{\partial t} - \frac{\nabla^2(\mathbf{B} - \mathbf{B}_0)}{\sigma\mu} + \frac{\mathrm{curl}(\mathbf{B} - \mathbf{B}_0)}{\sigma\mu} \times \frac{\nabla\sigma}{\sigma}. \tag{19}$$

7) Steady incompressible uniform neutral flow

An idealized flow that is steady, incompressible, neutral, and with uniform conductivity is analyzed in order to gain some physical insight. Its governing equations are:

$$\mathrm{div}(\mathbf{v} \times \mathbf{B}) = 0, \tag{20}$$

$$\mathrm{curl}(\mathbf{v} \times \mathbf{B}) = -\frac{\nabla^2(\mathbf{B} - \mathbf{B}_0)}{\sigma\mu}, \tag{21}$$

$$\mathrm{div}(\mathbf{v}) = 0, \tag{22}$$

$$\rho(\mathbf{v}\cdot\nabla\mathbf{v}) = -\nabla p + \mathrm{curl}(\frac{\mathbf{B} - \mathbf{B}_0}{\mu}) \times \mathbf{B}. \tag{23}$$

From (20) and (21) $\mathbf{v} \times \mathbf{B} = \mathrm{curl}(\mathbf{B} - \mathbf{B}_0)/\sigma\mu$. The cross product $-\mathbf{B} \times (\mathbf{v} \times \mathbf{B}) = -\mathbf{v}B^2 + \mathbf{B}(\mathbf{B}\cdot\mathbf{v})$ is the Lorentz force divided by the conductivity. The nonlinear velocity term in the momentum equation can be written as $\mathbf{v}\cdot\nabla\mathbf{v} = \nabla(v^2/2) - \mathbf{v} \times \mathrm{curl}(\mathbf{v})$. The vorticity $\mathrm{curl}(\mathbf{v})$ is zero by equation (22). Two expressions for the component of velocity transverse to the magnetic induction are found from the results just stated, and they are equated below,

$$\mathbf{v} - \mathbf{B}\frac{\mathbf{B}\cdot\mathbf{v}}{B^2} = \frac{-1}{\sigma B^2}\nabla(\frac{\rho v^2}{2} + p) = \frac{-\mathrm{curl}(\mathbf{B} - \mathbf{B}_0) \times \mathbf{B}}{\sigma\mu B^2}. \tag{24}$$

By using the vector relation shown above for $\mathbf{v}\cdot\nabla\mathbf{v}$ to expand $\mathbf{B} \times \mathrm{curl}(\mathbf{B})$ in equation (24), a Bernoulli theorem for this flow can be stated as

$$\nabla(\frac{\rho v^2}{2} + p + \frac{B^2}{2\mu}) = \frac{\mathbf{B}\cdot\nabla\mathbf{B}}{\mu} - \frac{\mathrm{curl}(\mathbf{B}_0) \times \mathbf{B}}{\mu}. \tag{25}$$

The total energy density of the fluid, a sum of kinetic, thermal, and magnetic contributions, changes along the flow as a result of sources of magnetic induction ($\mathbf{B}_0$), and gradients of the magnetic induction parallel to itself.

If the energy density is conserved ($\mathbf{B}_0 = 0$, $\mathbf{B}\cdot\nabla\mathbf{B} = 0$) then the magnitude of velocity at any point can be referred to conditions at a static origin, with initial conditions $p(\mathbf{r} = 0) = p_1$, and $B(\mathbf{r} = 0) = B_1$,

$$|v| = \sqrt{\frac{2}{\rho}[(p_1 - p) + \frac{B_1^2 - B^2}{2\mu}]}\,. \tag{26}$$

If there is no component of velocity parallel to the magnetic induction ($\mathbf{v} \perp \mathbf{B}$) then

$$\left|\frac{1}{\sigma B^2}\nabla\frac{B^2}{2\mu}\right| = \sqrt{\frac{2}{\rho}[(p_1 - p) + \frac{B_1^2 - B^2}{2\mu}]}\,. \tag{27}$$

Equation (27) gives B^2 as a function of position.

8) An axisymmetric flow

Consider an axisymmetric flow of the type described in section 7, with velocity and azimuthal induction as follows,

$$\mathbf{v} = v_r(r, z)\mathbf{i}_r + v_z(r, z)\mathbf{i}_z, \tag{28}$$

$$\mathbf{B} = B_\theta(r, z)\mathbf{i}_\theta. \tag{29}$$

Imagine that the electron beam pulse has heated and magnetized target material, which now expands to dissipate its initial energy density of $p_1 + {B_1}^2/2\mu$. Assume p quickly goes to zero close to the origin and all thermal energy becomes kinetic at a speed of v_T where ${v_T}^2 = 2p_1/\rho$. Assume that we are only interested in flow near the axis where $|v_r(r, z)| << |v_z(r, z)|$ and $B_\theta(r, z) \rightarrow B_\theta(z)$. An equation for $B_\theta(z)$ follows from equation (27) by assuming that positive $B_\theta(z)$ decays along negative coordinate z,

$$\frac{\partial B_\theta}{B_\theta\sqrt{(\rho\mu v_T^2 + B_1^2) - B_\theta^2}} = \frac{\sigma\mu}{\sqrt{\rho\mu}}\partial z\,. \tag{30}$$

If ${B_2}^2 = \rho\mu{v_T}^2 + {B_1}^2$ and ${z_M}^2 = (\rho\mu)/(\sigma\mu B_2)^2$, the integral of equation (30) is

$$\frac{1 + \sqrt{1 - \left(\frac{B_\theta}{B_2}\right)^2}}{\left(\frac{B_\theta}{B_2}\right)} = \frac{1 + \sqrt{1 - \left(\frac{B_1}{B_2}\right)^2}}{\left(\frac{B_1}{B_2}\right)} \exp\left(\frac{-z}{z_M}\right), \qquad (31)$$

and the corresponding velocity magnitude is given by equation (26),

$$|v| = \sqrt{v_r^2 + v_z^2} = \sqrt{\frac{B_2^2 - B_\theta^2}{\rho\mu}}. \qquad (32)$$

Recall that we have assumed this velocity magnitude to be primarily that of the axial component. Equation (22) for continuity requires a radial velocity component as this is a constant density flow that accelerates axially.

It is probably best to apply these results only within an axial extent comparable to the diameter of the electron beam, where both cylindrical and spherical flows would be similar and the variation in density may not be too drastic.

9) Two examples

Figure 1 shows the axial variation of $B_\theta(z)$ from equation (31), and velocity magnitude $|v(z)|$ from equation (32) for example 1, which has the following parameters: conductivity $\sigma = 8 \times 10^4$ Siemens/m, density $\rho = 8 \times 10^{-3}$ kg/m^3, thermal velocity $v_T = 1$ km/s, and an initial magnetic induction of $B_\theta(0) = B_1 = 1$ Tesla. The scale length for this acceleration is $z_M = 1$ mm, and it reaches a velocity magnitude of $|v(-3z_M)| = 10$ km/s. The magnetic diffusion time based on length scale z_M is $\sigma\mu z_M^2 = 100$ ns.

Example 2 differs from the previous example in that $\sigma = 8 \times 10^3$ Siemens/m and $\rho = 8 \times 10^{-5}$ kg/m^3. In this case the final velocity magnitude is $|v(-3z_M)| = 100$ km/s, the scale length for the acceleration is again $z_M = 1$ mm, and the characteristic diffusion time is $\sigma\mu z_M^2 = 10$ ns. The axial variations of $B_\theta(z)$ and $|v(z)|$ look the same as those of Figure 1, except that magnitude $|v(-3z_M)|$ is ten times higher for example 2. **Figure 2** shows the elapsed time to a distance,

assuming the velocity magnitude is purely axial, for example 1 at the top and example 2 below.

Fully ionized plasma with a temperature of 11 eV will have a Spitzer (1962) conductivity [ln(Λ) = 8.8] equal to that of example 1; for example 2 the equivalent temperature is 2.4 eV. Assuming the flows are copper, the particle densities for examples 1 and 2, respectively, are 8×10^{16} cm^{-3} and 8×10^{14} cm^{-3}.

10) Rules-of-thumb

The previous examples can hardly encompass the involved process of heating, magnetizing, and accelerating target material simultaneously by electron beam impact. However, they do suggest some rules-of-thumb for estimating the properties of matter accelerated electromagnetically — assuming this occurs at the target.

The maximum flow velocity can be estimated from equation (32), and is seen to be a combination of the thermal and Alfvén velocities based on initial conditions,

$$|v| \le \sqrt{\frac{B_1^2}{\rho\mu} + v_T^2} = \sqrt{v_A^2 + v_T^2}. \tag{33}$$

The flows of greatest interest are those with $v_A^2 >> v_T^2$. For such flows the scale length of the acceleration, as modeled in section 8, is

$$z_M = \frac{\sqrt{\rho\mu}}{\sigma\mu B_1} = \frac{1}{\sigma\mu v_A}. \tag{34}$$

The time scale for the magnetic field lines in the material to diffuse away is comparable to the time scale for the material to accelerate electromagnetically. This characteristic diffusion time is

$$t_M = \sigma\mu z_M^2. \tag{35}$$

From (33)—(35) we can deduce several equivalent expressions for v_A,

$$v_A = \frac{1}{\sigma\mu z_M} = \frac{B_1}{\sqrt{\rho\mu}} = \frac{z_M}{t_M}. \qquad (36)$$

The first of the expressions in equation (36) can be written as the magnetic Reynolds number, a dimensionless product here equal to one,

$$R_M = \sigma\mu v_A z_M = 1. \qquad (37)$$

The magnetic field changes over time in high magnetic Reynolds number flow by being swept along with the motion. Magnetic diffusion controls the rate of change of the magnetic field when R_M is much less than unity. Diffusion and transport of magnetic field lines are comparable effects when R_M is near unity. It seems reasonable to expect the electromagnetic acceleration of target material to be a flow with $R_M = 1$. The effect of magnetic Reynolds number can be seen mathematically by transforming equation (13), for the evolution of $\mathbf{B}(\mathbf{r}, t)$, into a dimensionless form.

The practical conclusion of this analysis is that equations (36) and (37) can be used as rules-of-thumb for estimating how material density ρ, electrical conductivity σ, initial magnetization B_1, and scale length z_M influence the velocity achieved by electromagnetic acceleration when $|v| = v_A >> v_T$.

11) Magnetizing the target

Is it possible to magnetize the target during the course of a single pulse? If electromagnetic acceleration is to occur then a large magnetic induction must be infused into the target during the 50 ns to 100 ns period of the pulse. Diffusion of the vacuum field of the electron beam into the solid target is too slow, the diffusion time $\sigma\mu L^2$ is longer than the pulse. Rapid magnetizing can occur by a thermal electric effect. The large temperature gradient, generated as a result of the radial profile of the electron beam, can produce a significant magnetic field in the target during the course of a single pulse. The spontaneous generation of magnetic fields by collisional and thermal electric effects is described in a recent report, see Reference 12.

Consider static, neutral, conducting material at constant density. Equation (17) for momentum reduces to a balance between the pressure gradient and the Lorentz force, $\nabla p = \mathbf{j} \times \mathbf{B}$. By using $p = kNT$ and $\mathbf{j} = \text{curl}(\mathbf{B} - \mathbf{B}_0)/\mu$, where $k = 1.38054 \times 10^{-23}$ J/°K and the particle density N is uniform, then

$$\mathbf{j} = \frac{kN(\mathbf{B} \times \nabla T)}{B^2} - \frac{\mathbf{B}(\mathbf{B} \cdot \mathbf{j})}{B^2}. \tag{38}$$

The pressure gradient, in this case a temperature gradient in uniform material, causes a current to flow transverse to the magnetic induction. This thermal electric current is called a "Nernst term" in Reference 12, where it is noted that "Nernst convection of the magnetic field by the heat flux…can result in a local magnification of the field." **Figure 3** shows an example of isotherms in a target.

A single species, ideal fluid model is inadequate to simulate the simultaneous heating and magnetizing of the target by an electron beam. To include effects such as Nernst convection it is better to use a multi-species model with a "generalized Ohm's law" in place of equation (7) for the current density. References 12—16 each describe the generalized Ohm's law. The single species, ideal fluid model is used in this section to keep the discussion simple.

Assume our idealized magnetizing occurs with a conductivity that depends only on temperature so that $\nabla\sigma \parallel \nabla T$, and also assume that $\mathbf{j} \perp \mathbf{B}$ and $\mathbf{j} \perp \nabla\sigma$. The vectors $\mathbf{B}$, ∇T, and $\mathbf{j}$ are arranged like a bicycle wheel: $\mathbf{B}$ is along the hub, ∇T are the spokes, and $\mathbf{j}$ is the rim and tire. Equation (19) gives the evolution of $\mathbf{B}$ with a non-uniform conductivity as assumed here,

$$\frac{\partial \mathbf{B}}{\partial t} = \frac{\nabla^2(\mathbf{B} - \mathbf{B}_0)}{\sigma\mu} + \frac{kN(\nabla\sigma \cdot \nabla T)}{(\sigma B)^2}\mathbf{B}. \tag{39}$$

The rate of change of $\mathbf{B}$ is due to leakage through the material and a thermal electric source. The ratio of the thermal electric term to the leakage term has a magnitude comparable to the ratio of thermal to magnetic pressure

$$\beta = \frac{2\mu k N \Delta T}{B^2} \tag{40}$$

when **B** varies on the same length scale as the temperature difference ΔT. The thermal electric term will overwhelm the leakage term during the pulse because of the combined effects of a large temperature gradient and a high density.

An estimate of the rate-of-rise of B at early times follows from (39) by ignoring the leakage term and assuming the thermal electric parameters are steady,

$$B = \sqrt{\frac{2 k N \Delta T t}{\sigma L^2}} \ . \tag{41}$$

If $N = 8.5 \times 10^{28}$ m^{-3}, $\Delta T = 11605$ °K, $\sigma = 5.8 \times 10^7$ S/m, and $L = 10^{-3}$ m then $B = 1$ T in 2 ns. In this example N and σ are the density and conductivity of solid copper, while ΔT is a temperature difference of 1 eV. The magnetic diffusion time for this example is 73 μs, and the ratio $\beta = 3.4 \times 10^4$ with $B = 1$ T. Steady state has $B = 185$ T for $\beta = 1$.

The slow leakage of thermally generated high magnetic field to the surface of the plate may propel low density conducting material to high speed.

12) Conclusions

1) The target quickly magnetizes by the thermal electric effect because the electron beam creates large axial and radial temperature gradients.

2) The leakage of magnetic field is slow because of the high conductivity.

3) Electromagnetic acceleration can propel low density material to high speed as the electron beam pulse decays.

4) Electromagnetic acceleration occurs as a $R_M = \sigma\mu v L = 1$ flow.

5) Beam-in-target simulations may show superthermal outflow.

Appendix: steady incompressible charged flow

This appendix will describe how a charge source $\rho_0(\mathbf{r}, t)$ can affect the flow. Charged flow is the counterpart to ion backstreaming (see References 1—3) from the perspective of this ideal fluid model. By now both the limitations of the model and conclusions about electromagnetic acceleration have been stated, here we simply continue discussing the equations within the same context.

The governing equations here are:

$$\operatorname{div}(\mathbf{v} \times \mathbf{B}) = \frac{-\rho_0}{\varepsilon} - \frac{\operatorname{curl}(\mathbf{B} - \mathbf{B}_0)}{\sigma\mu} \cdot \frac{\nabla\sigma}{\sigma}, \tag{18}$$

$$\operatorname{curl}(\mathbf{v} \times \mathbf{B}) = \frac{-\nabla^2(\mathbf{B} - \mathbf{B}_0)}{\sigma\mu} + \frac{\operatorname{curl}(\mathbf{B} - \mathbf{B}_0)}{\sigma\mu} \times \frac{\nabla\sigma}{\sigma}, \tag{42}$$

$$\operatorname{div}(\mathbf{v}) = 0, \tag{22}$$

$$\rho(\mathbf{v}\cdot\nabla\mathbf{v}) = -\nabla p + \operatorname{curl}(\frac{\mathbf{B} - \mathbf{B}_0}{\mu}) \times \mathbf{B}. \tag{23}$$

Recall that $\mu\mathbf{j} = \operatorname{curl}(\mathbf{B} - \mathbf{B}_0)$. Assume that $\mathbf{j} \perp \nabla\sigma$ and that $\sigma\mu L^2$ is large, so that $\operatorname{curl}(\mathbf{v} \times \mathbf{B}) = 0$. With these assumptions the system reduces to:

$$\operatorname{div}(\mathbf{v} \times \mathbf{B}) = \frac{-\rho_0}{\varepsilon}, \tag{12}$$

$$\mathbf{v} \times \mathbf{B} = \nabla\phi\ , \tag{43}$$

$$\nabla(\frac{\rho v^2}{2} + p + \frac{B^2}{2\mu}) = \frac{\mathbf{B}\cdot\nabla\mathbf{B}}{\mu} - \mathbf{j}_0 \times \mathbf{B}. \tag{25}$$

The charge source ρ_0 establishes an electrostatic field $-\nabla\phi$, and flow is a $-\nabla\phi \times \mathbf{B}$ drift. Assume that $\mathbf{v} \perp \mathbf{B}$, $\mathbf{j}_0 \perp \mathbf{B}$, and $\mathbf{B}\cdot\nabla\mathbf{B} = 0$; and define the energy density as

$$U = \frac{\rho v^2}{2} + p + \frac{B^2}{2\mu}. \tag{44}$$

The effect of the current source is to produce a gradient of energy density $\nabla U = -\mathbf{j}_0 \times \mathbf{B}$; for example, an axial current source and an azimuthal magnetic induction are a Lorentz force equivalent to a radial energy density gradient. The velocity and magnetic induction here are seen to be:

$$\mathbf{v} = \frac{\mathbf{B} \times \nabla\phi}{B^2}, \tag{45}$$

$$\mathbf{B} = \frac{\mathbf{j}_0 \times \nabla U}{\mathrm{j}_0^2}. \tag{46}$$

The velocity is reduced to a more primitive form by eliminating **B**,

$$\mathbf{v} = -\mathbf{j}_0 \frac{(\nabla\phi \cdot \nabla U)}{|\nabla U|^2}. \tag{47}$$

This shows a velocity in the direction opposite of the current source (parallel to an electron beam) if the gradients in electrostatic potential and energy density are parallel. If we imagine that pressure has a strong gradient while both the kinetic and magnetic energy densities are fairly uniform, then ∇U is given by the temperature gradient, and the velocity is

$$\mathbf{v} = -\mathbf{j}_0 \frac{(\nabla\phi \cdot \nabla T)}{\mathrm{k}N|\nabla T|^2}. \tag{48}$$

The following example provides one estimate of a velocity from equation (48). A positive charge density $\rho_0 = \mathrm{e}n_0 = 16$ C/m^3 has a source particle density $n_0 = 10^{14}$ cm^{-3}. A current density source $\mathbf{j}_0 = -\rho_0 \mathrm{c}\mathbf{i}_z = -(5 \times 10^9)\mathbf{i}_z$ A/m^2 has an equivalent charge density of relativisitic electrons moving along positive $\mathbf{i}_z$. Gradients occur over a radial extent of $L = 10^{-3}$ m. The average gradient of the electrostatic potential is estimated as $\nabla\phi = -(1/4)(\rho_0 L/\varepsilon)\mathbf{i}_r = -(4.5 \times 10^8)\mathbf{i}_r$ V/m. A temperature drop of 8.6 eV over L is equivalent to a gradient of $\nabla T = -(10^8)\mathbf{i}_r$ °K/m. For density $N = 8.5 \times 10^{28}$ m^{-3} the velocity is $\mathbf{v} = (2 \times 10^4)\mathbf{i}_z$ m/s $= (2)\mathbf{i}_z$ cm/μs.

In this case $B = 2 \times 10^4$ T. If pressure at 8.6 eV were all converted to magnetic flux then $B = 543$ T. This discrepancy only underscores the limitations of the model and the cumulative inaccuracy of all the assumptions. See the discussion and citations in Reference 12 to appreciate the scope of a complete model.

Without a charge source there is no motion in the last example, it reduces to a static thermal electric balance, as in equations (38) or (46). The magnetic induction **B** is in the opposite sense of the source magnetic induction $\mathbf{B}_0$, and it is larger. The direction of the charged flow is with the electron beam because both the potential and the temperature increase toward the axis.

This model suggests that positive charge on the target at the entry point of the electron beam may be restrained by a large magnetic field generated thermally.

References

1) P. W. Rambo and S. Brandon, "e-beam interaction with field emitted ions from bremsstrahlung targets," Lawrence Livermore National Laboratory, Memorandum, 29 April 1997.

2) T. J. T. Kwan, J. C. Goldstein, B. G. DeVolder, "Influence of ions on electron beam spot size in ITS/DARHT," Los Alamos National Laboratory, XPA-RN(U) 97-021, 9 June 1997.

3) T. J. T. Kwan and C. M. Snell, "Stabilization of radiographic spot size via self-biasing targets," Los Alamos National Laboratory, XPA-RN(U) 97-048, 12 November 1997.

4) Hydrodynamic calculations by P. Pincosy with CALE, and D. Ho with LASNEX, Lawrence Livermore National Laboratory.

5) B. G. DeVolder, T. J. T. Kwan, R. D. Fulton, D. C. Moir, D. M. Oro, D. S. Prono, "Computational and experimental studies of the beam-target interaction for high-dose, multi-pulse radiography," Los Alamos National Laboratory, LA-UR-97-8, and the 24TH IEEE International Conference on Plasma Science, 7P26, 19-22 May 1997, San Diego, CA.

6) B. G. DeVolder, T. J. T. Kwan, K. D. McLenithan, "Computational and experimental studies of the beam-target interaction for x-ray radiography," Los Alamos National Laboratory, XPA-RN(U) 97-049, 19 November 1997.

7) M. Garcia, "Splash flow from a metal plate hit by an electron beam pulse," Lawrence Livermore National Laboratory, UCRL-ID-128660, 4 September 1997.

8) M. Garcia, "Frozen plasma within the flow from a metal plate hit by an electron beam pulse," Lawrence Livermore National Laboratory, UCRL-ID-126296, 12 November 1997.

9) W. Wood et al., "Dynamic measurements of plasmas generated by relativistic electrons colliding with metal targets," to be presented at the IEEE International Conference on Plasma Science (ICOPS) '98, Raleigh, North Carolina, 1—4 June 1998.

10) M. Garcia, "Magnetized plasma ejected from metal targets during pulsed electron beam impact," Lawrence Livermore National Laboratory, UCRL-ID-129690, 15 January 1998. This report is the product of enthusiasm, intuition, and far too much speculation. Its value was in initiating the author's present study of electromagnetic acceleration from electron beam targets.

11) J. H. M. M. Schmitt, "Stellar Coronae," in *Stellar Atmospheres: Theory and Observations*, J. P. De Greve, R. Blomme, H. Hensberge (Eds.), Berlin: Springer-Verlag, 1997.

12) W. E. Alley, "The effects of self-induced magnetic fields in laser-produced titanium plasmas," Lawrence Livermore National Laboratory, UCRL-JC-128092, 18 July 1997. This paper was prepared for submittal to Physical Review Letters.

13) F. F. Chen, *Introduction to Plasma Physics*, New York: Plenum Press, 1974, see section 5.7, "The single-fluid MHD equations."

14) B. S. Tanenbaum, *Plasma Physics*, New York: McGraw-Hill Book Company, 1967, see section 3.10, "The nonlinear MHD equations."

15) E. H. Holt and R. E. Haskell, *Foundations of Plasma Dynamics*, New York: The Macmillan Company, 1965, see section 6.51, "The generalized Ohm's law."

16) M. Mitchner and C. H. Kruger, Jr., *Partially Ionized Gases*, New York: John Wiley & Sons, 1973, see chapter 4, section 8, "Magnetohydrodynamics; The generalized Ohm's law," and chapter 8, section 4, "Transport properties; Patially ionized plasmas."

Figure legends

1) **Axial variation of example 1.** $B_\theta(z)/(B_1 = 1$ Tesla) and $|v(z)|$ when $\sigma = 8 \times 10^4$ Siemens/m, $\rho = 8 \times 10^{-3}$ kg/m^3, and $v_T = 1$ km/s. The scale length is $z_M = 1$ mm, the characteristic diffusion time is $\sigma\mu z_M^2 = 100$ ns, and the terminal speed is $|v(-3z_M)| = 10$ km/s.

2) **Elapsed time to distance.** Assumes the velocity magnitude is purely axial; for example 1 at the top, and example 2 below. Example 2 has $\sigma = 8 \times 10^3$ Siemens/m and $\rho = 8 \times 10^{-5}$ kg/m^3; B_1 and v_T as before. $z_M = 1$ mm, $\sigma\mu z_M^2 = 10$ ns, and $|v(-3z_M)| = 100$ km/s for example 2. The axial variations look the same as Figure 1 except $|v(-3z_M)|$ is ten times higher for example 2.

3) **Isotherms at the end of a pulse.** This drawing is based on a calculation by P. Pincosy of LLNL. A 1 mm FWHM, 20 MeV, 6 kA electron beam of 60 ns duration traverses a 1 mm thick tantalum plate. The dashed lines show the edge of the beam. Isotherms may also be surfaces of constant pressure, conductivity, and charge. Strong temperature gradients generate large magnetic fields from thermally driven currents. Slow magnetic leakage may propel low density surface plasma to superthermal speed.

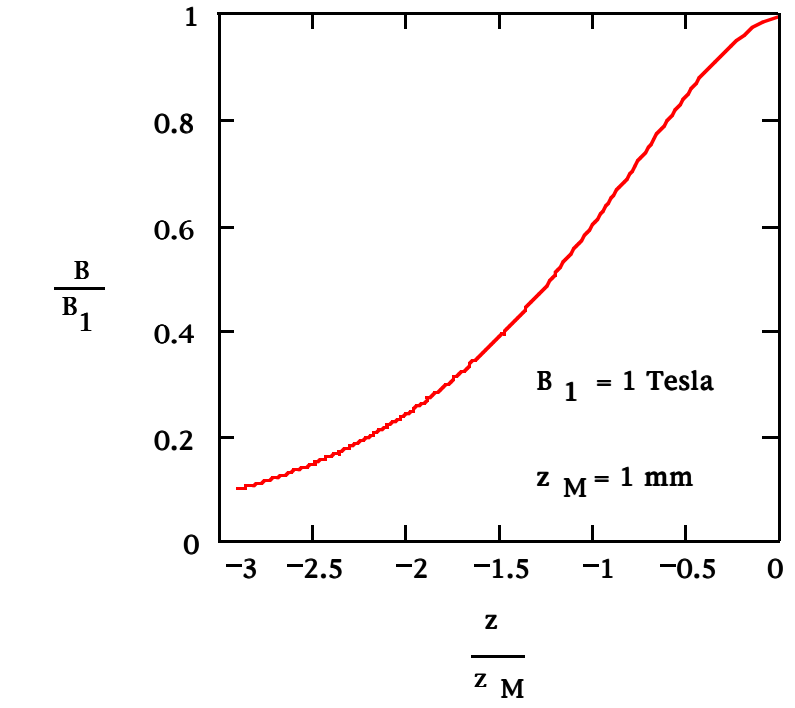

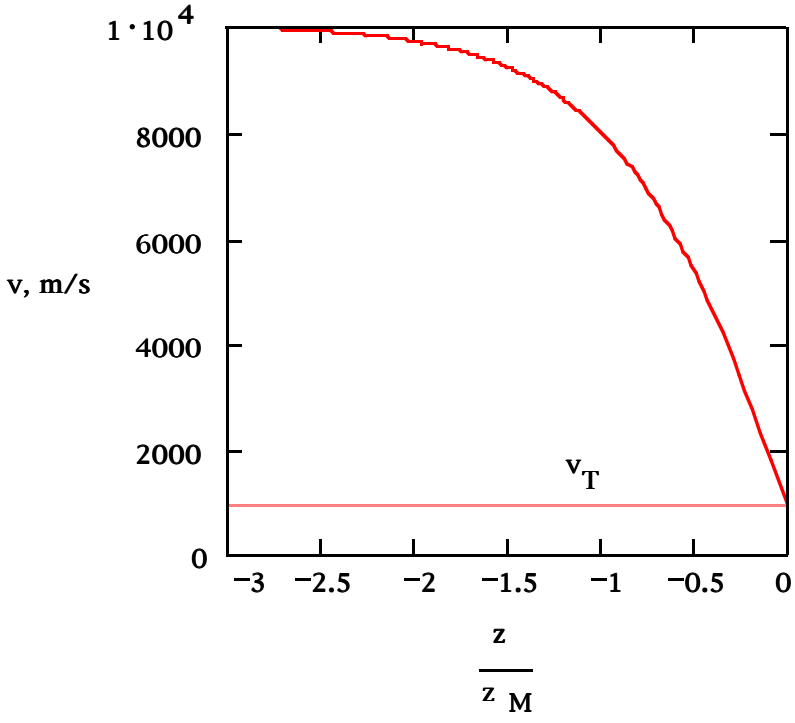

Figure 1. Axial variation of example 1

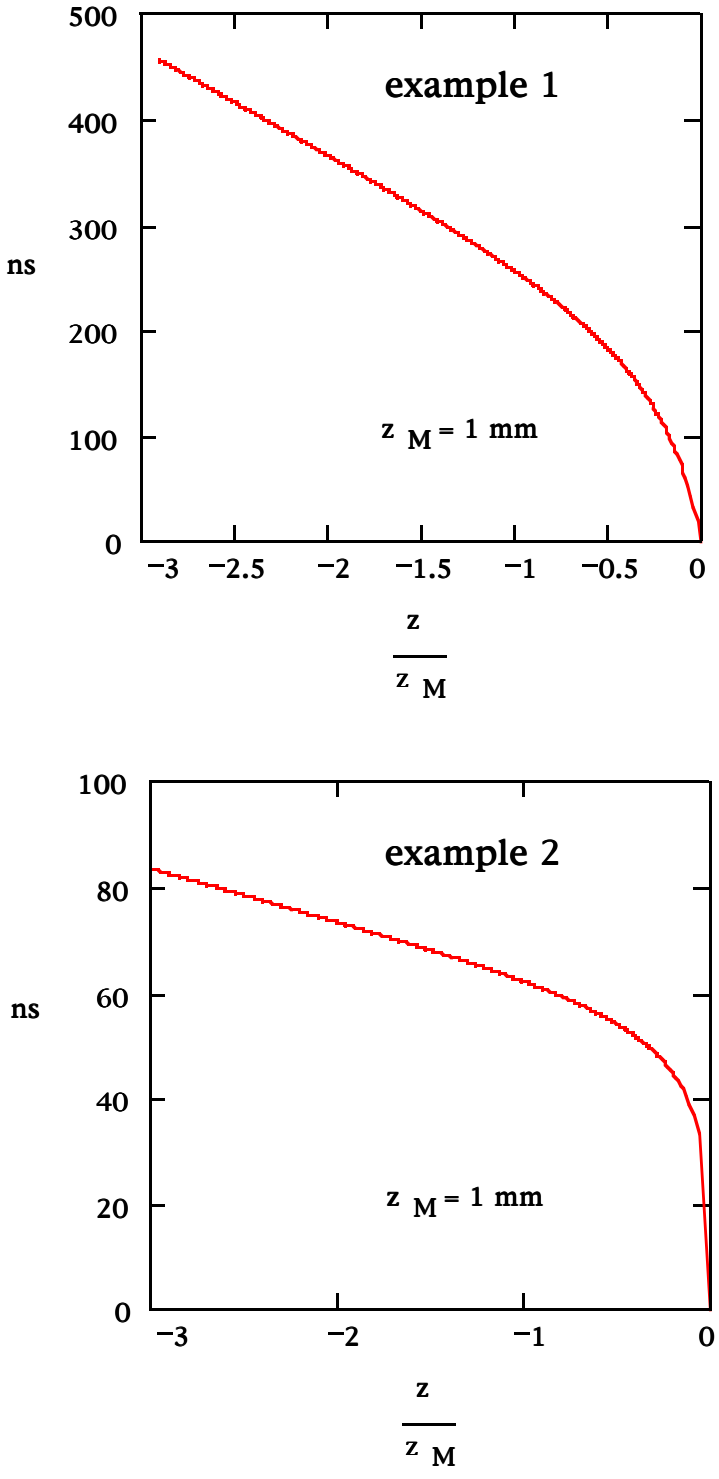

Figure 2. Elapsed time to distance.

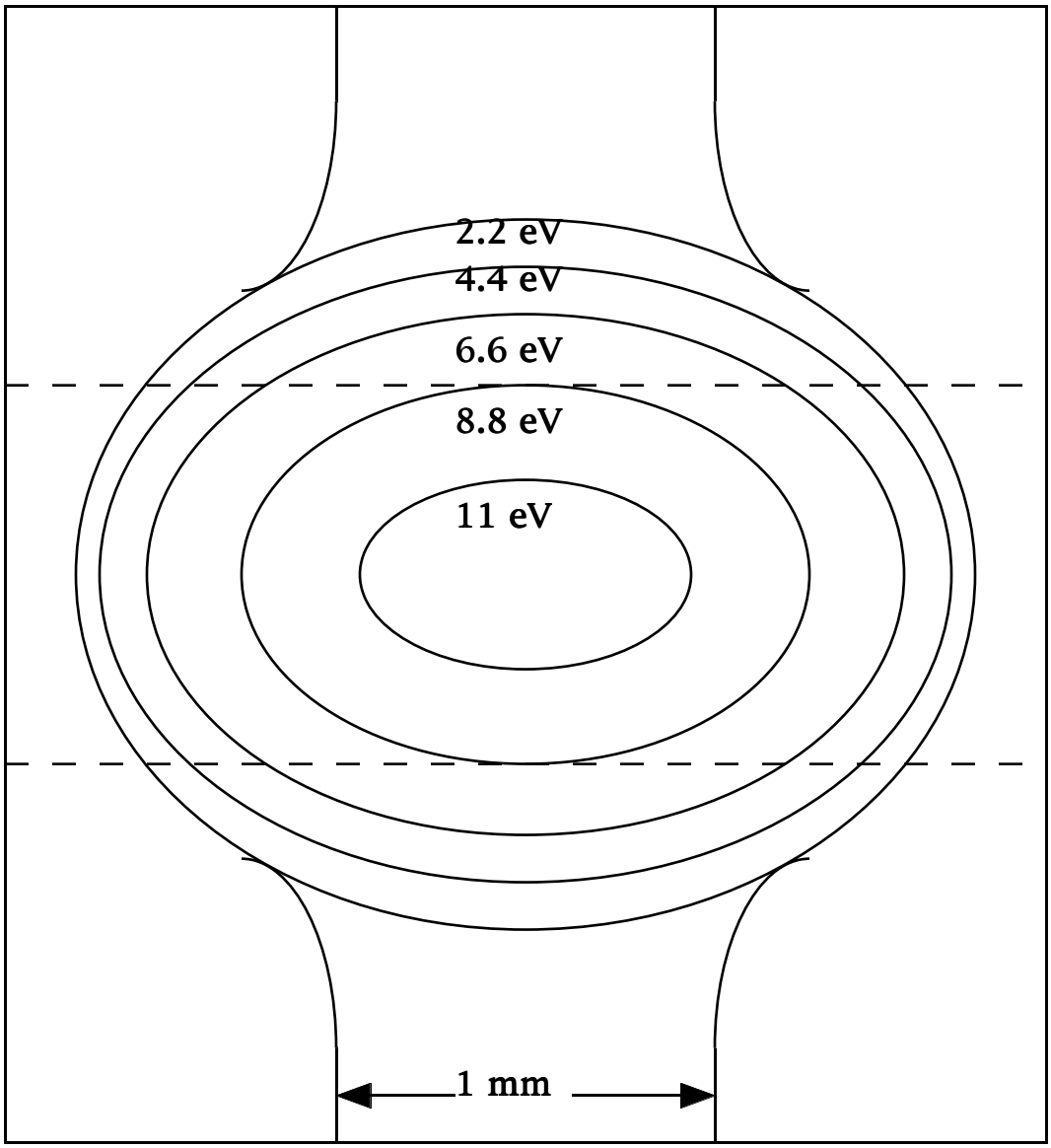

Figure 3: Isotherms at the end of a pulse
(courtesy of P. Pincosy, LLNL, April 1998)

Technical Information Department • **Lawrence Livermore National Laboratory**
University of California • Livermore, California 94551